Single-End-Access Correlation-Domain Distributed Fiber-Optic Sensor Based on Stimulated Brillouin Scattering

Weiwen Zou, *Member, IEEE, OSA*, Zuyuan He, *Member, IEEE, OSA*, and Kazuo Hotate, *Fellow, IEEE*

***Abstract*—We propose a single-end-access correlation-domain distributed fiber-optic sensor based on stimulated Brillouin scattering (SBS) in a polarization-maintaining optical fiber (PMF). Frequency-modulated pump and probe waves are launched into the same end of the PMF with orthogonal polarization states. Assisted by a polarization beam splitter and a polarization-maintaining isolator installed at the other end of the PMF, SBS interaction between the reflected probe wave and the forward pump wave is exclusively localized within the PMF. Unlike the previously-reported method based on placing a reflector at the far end of the fiber (Song *et al.*, 2008), in which the measurement range is shortened to a half of the nominal value determined by the frequency modulation, as given in the work by Hotate and Hasegawa (2000), our new method maintains the range as the nominal value. Distributed sensing of temperature or strain is experimentally demonstrated with the measurement range/the spatial resolution of 200 m/16 cm, 56 m/5 cm, or 5.6 m/5 mm, respectively.**

***Index Terms*—Fiber optic sensors, polarization-maintaining fiber, scattering measurements, stimulated Brillouin scattering (SBS).**

I. Introduction

FIBER-OPTIC distributed sensors based on Brillouin scattering [1]–[6] have been extensively studied during the past decades because they are regarded as powerful tools for measuring temperature or strain distribution in smart materials and smart structures. Brillouin scattering occurring in the fiber under test or the fiber as a sensing element is physically attributed to the interaction between optical photons and acoustic phonons. The frequency of the scattered (or amplified) photons is downshifted from that of the incident (or pump) photons. The downshifted frequency is known as Brillouin frequency shift (BFS, ν_{B}) and is proportional to the acoustic velocity in the sensing fiber. Either temperature or strain change alters linearly the acoustic velocity [7], [8], so that the temperature or strain information can be obtained by monitoring the BFS ν_{B}.

To obtain the position information for distributed sensing, i.e., to resolve the Brillouin scattering from different positions along the fiber, various techniques have been developed, for example, the pulse-based technique [1]–[3] or the continuous-wave correlation-based technique [4]–[6]. The pulse-based technique has the advantage of long-length measurement ability ($\sim$tens of kilometers), while the correlation-based technique has unique features of random-access ability and high spatial resolution (even sub-centimeter).

Both the spontaneous Brillouin scattering (SpBS) and the stimulated Brillouin scattering (SBS) are utilized for distributed sensing. SpBS is used to build single-end-access distributed sensor [3], [6], called Brillouin optical time-domain reflectometry (BOTDR) or Brillouin optical correlation-domain reflectometry (BOCDR), respectively, which is more flexible in long-length measurement application but with much weaker signal compared to SBS-based sensors. SBS-based sensors, on the other hand, can provide much stronger signals, but need double-end-access to the fiber since pump and probe waves need to counter-propagate along the fiber [1], [4], [5]. Recently, a single-end-access SBS-based distributed sensor with continuous-wave correlation-domain technique was proposed, in which a reflector is placed at the far end of the sensing fiber to reflect the forward pump and probe waves back, and SBS is generated by the interaction between the backward waves and the forward waves [9]. The drawback of above configuration is that, due to the two-folding of the optical path, there are two cases of SBS interaction at different positions at a moment, and then the usable measurement range is shortened to a half of the nominal value of the correlation-domain technique [4].

In this paper, we propose a novel scheme of a single-end-access correlation-domain SBS-based fiber-optic distributed sensor. A polarization-maintaining optical fiber (PMF) is used as the sensing element. Using the PMF allows ideal SBS interaction when Brillouin pump and probe waves polarized with the same axis (slow or fast). Recently, a new concept of Brillouin dynamic grating in PMF was demonstrated [10], which is attributed to the facts that the acoustic wave generated in SBS is a longitudinal-wave and that the high birefringence of a PMF does not differentiate the acoustic waves [11]. The Brillouin dynamic grating in a PMF enables a complete discrimination of strain and temperature in SBS-based distributed sensors

Manuscript received March 08, 2010; revised June 20, 2010; accepted July 21, 2010. Date of publication July 29, 2010; date of current version September 03, 2010. This work was supported by the "Grant-in-Aid for Scientific Research (S)" and the "Global Center of Excellence Program" from the Ministry of Education, Culture, Sports, Science and Technology (MEXT), Japan.

W. Zou was with the Department of Electrical Engineering and Information Systems, The University of Tokyo, Tokyo 113-8656, Japan. He is now with the State Key Laboratory of Advanced Optical Communication Systems and Networks, the Department of Electronic Engineering, Shanghai Jiao Tong University, Shanghai 200240, China (e-mail: wzou@sjtu.edu.cn).

Z. He and K. Hotate are with the Department of Electrical Engineering and Information Systems, The University of Tokyo, Tokyo 113-8656, Japan (e-mail: ka@sagnac.t.u-tokyo.ac.jp, hotate@sagnac.t.u-tokyo.ac.jp).

Color versions of one or more of the figures in this paper are available online at http://ieeexplore.ieee.org.

Digital Object Identifier 10.1109/JLT.2010.2062172

0733-8724/$26.00 © 2010 IEEE

[12]–[15]. It was also demonstrated that sub-meter spatial resolution can be realized in Brillouin time-domain distributed sensing by use of the Brillouin dynamic grating in a PMF [16], [17]. In the proposed configuration of the single-end-access SBS-based distributed sensor, the SBS interaction is limited to one position of the sensing PMF at a moment, so the measurement range is not halved as in previously reported scheme based on an inline reflector [9]. The frequency modulation depth, which determines the spatial resolution in the correlation-domain technique, can far exceed a half of the BFS ν_{B} in the new scheme without the necessity of the optical filter and the sophisticated beat-lock-in detection required in [9], and thus higher spatial resolution can be realized easier. We demonstrate experimentally single-end-access distributed sensing of temperature or strain with three different alternatives of the measurement range to the spatial resolution $(d_{\mathrm{m}}/\Delta z)$ of 200 m/16 cm, 56 m/5 cm, or 5.6 m/5 mm, respectively.

II. Principles

Two different schemes of single-end-access SBS-based fiber-optic distributed sensors, that is, the previous scheme based on an inline reflector [9] and the novel scheme proposed in this paper, are compared in Fig. 1. In Fig. 1(a), sinusoidally frequency-modulated pump and probe waves are both launched into a single-mode optical fiber (SMF) from one end (the near end) [9]. One of the forward waves is reflected back by a reflector laid at the other end (the far end) of the SMF. The reflected wave encounters the other forward wave generating SBS at a particular position corresponding to the correlation peak due to their sinusoidal frequency modulation. There are two cases of SBS interaction between the reflected probe (pump) and the forward pump (probe) waves as shown in Fig. 1(a) [9]. This condition shortens the measurement range to a half of the nominal value of the correlation-domain technique such as that in traditional Brillouin optical correlation domain analysis (BOCDA) system [4].

The novel scheme is depicted in Fig. 1(b). A polarization-maintaining optical fiber (PMF) is used as the sensing element. Sinusoidally frequency-modulated pump and probe waves are linearly polarized with the same polarization state [x-oriented in Fig. 1(b)]. The pump and probe waves are both incident into the near end of the PMF through a polarization-beam splitter/combiner (PBS/C1) and propagate along the PMF with the orthogonal polarization states (pump, x -oriented; probe, y-oriented). Another PBS/C (PBS/C2) is installed at the far end of the PMF. The y-oriented probe wave enters PBS/C2, passes through a polarization-maintaining isolator (PM-ISO), and finally returns to PBS/C2 in x-orientation. Consequently, the backward probe wave encounters the forward pump wave with the same polarization state (x-oriented) and thus SBS occurs exclusively. Since there is only one case of SBS interaction between x-oriented forward pump wave and x-oriented backward probe wave, the measurement range (d_{m}) is exactly the same as the traditional two-end-access BOCDA system [4], and so is the spatial resolution (Δz), given by

$$d_m = \frac{c}{2n_{\mathrm{eff}} f_m} \tag{1}$$

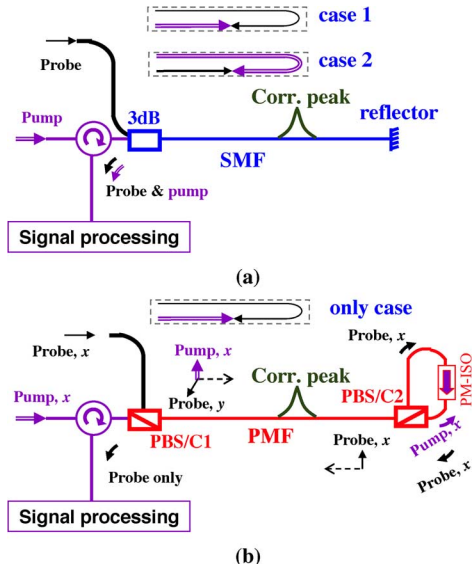

Fig. 1. Comparison of two different schemes of single-end-access SBS-based distributed sensors based on (a) a reflector and (b) a combined PBS and PM-ISO installed at the far end of the sensing fiber. There are two cases of SBS interaction in (a) but only one in (b).

$$\Delta z = d_m \frac{\Delta \nu_B}{\pi \Delta f} \tag{2}$$

where c is the light speed in vacuum, n_{eff} (~ 1.446) the effective refractive index of the PMF, $\Delta\nu_{\mathrm{B}}$ the Brillouin linewidth ($\sim$30 MHz), f_{m} the modulation frequency, and Δf the modulation depth, respectively.

Furthermore, in the new scheme, only SBS-amplified probe wave appears in the photo-detector, while both pump and probe waves do in the previous reflector-based scheme [9]. Therefore, the novel scheme simplifies the signal processing as compared to the reflector-based scheme. Since the forward pump wave is completely blocked by the PM-ISO, the pump wave and the Brillouin loss at the pump frequency appearing in the output are only related to the crosstalk of the PMF ($\gamma < -25$ dB/100 m). The detected output (P_{d}) can be expressed by:

$$\begin{aligned} P_d &= P_s e^{gP_p \Delta z/A_{\mathrm{eff}}} + \gamma \left(P_p - P_s e^{gP_p \Delta z/A_{\mathrm{eff}}} \right) \\ &\approx \gamma P_p + (1-\gamma) P_s + (1-\gamma) g P_p P_s \Delta z / A_{\mathrm{eff}} \end{aligned} \tag{3}$$

where $g =\sim 1.7 \times 10^{-11}$ m/W is the Brillouin gain coefficient [18], $A_{\mathrm{eff}} =\sim 100\ \mu\mathrm{m}^2$ the effective area of the PMF [11], and P_s (P_p) the input power of the probe (pump) wave, respectively. As demonstrated in next section, a single-lock-in detection that was employed in the traditional BOCDA system [4] is sufficient to demodulate the Brillouin interaction (gain) signal, i.e., the third component of the right-hand side of (3). It is not necessary to use an optical filter to cut down the pump wave and the Brillouin loss signal at the frequency of the pump wave because its influence to the Brillouin gain is negligible (< -25 dB), which is superior to the reflector-based scheme [9] or the SpBS-based BOCDR [6]. It is noted that when the frequency modulation depth exceeds a half of the BFS $(\Delta f > \nu_{\mathrm{B}}/2)$, the spectra at the frequencies of the Brillouin pump and probe waves start to overlap between different frequency components. The pump

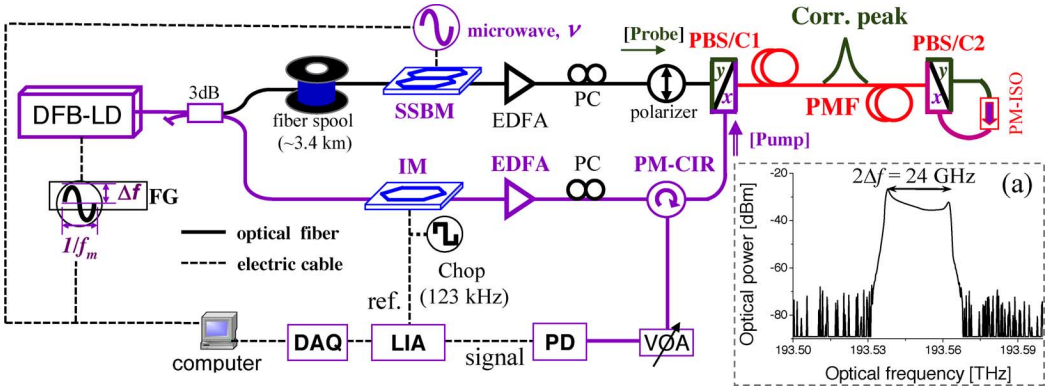

Fig. 2. Experimental setup of the single-end-access SBS-based correlation-domain distributed sensor. The inset (a) shows the optical power spectrum of the frequency-modulated laser source with a modulation depth $\Delta f =\sim 12$ GHz. All the abbreviations are explained in the text body.

wave (including the Brillouin loss signal in the reflector-based scheme or the Rayleigh scattering in the SpBS-based BOCDR) can not be distinguished from the overlapped spectra even by using any optical filter. In the new scheme, due to the complete isolation of the pump wave at the far end of the sensing PMF, there is no limitation of the modulation depth, which ensures more achievable spatial resolution than the reflector-based scheme [9] and also than the SpBS-based BOCDR [6].

III. Experimental Details

A. Experimental Setup

The experimental setup is illustrated in Fig. 2. A 1549-nm distributed-feedback laser diode (DFB-LD) was used as the laser source, and a sinsodinal frequency modulation was directly applied by a function generator (FG). The inset of Fig. 2 shows the optical power spectrum of the frequency-modulated laser source with the modulation depth $\Delta f =\sim 12$ GHz, which is even greater than the BFS $\nu_{\rm B} =\sim 10.9$ GHz of the PMF. The output of the DFB-LD was divided by a 3-dB coupler to generate pump and probe waves, respectively. A single-sideband modulator (SSBM) driven by a mirowave synthesizer was used to downshift and sweep the optical frequency of the probe wave around the BFS $\nu_{\rm B}$. Due to the sinusoidal frequency modulation, a series of periodical correlation peaks were produced. A $\sim$3.4-km SMF spool was laid in the probe arm to introduce a higher-order correlation peak within the PMF, hence the SBS interaction was localized at the correlation peak position. An intensity modulator (IM) was employed to chop the pump power at a frequency of 123 kHz. Pump and probe waves were amplified by two erbium-doped fiber amplifers (EDFAs) to $\sim$24 dBm and $\sim$7 dBm, respectively. The probe and pump waves were linearly polarized by a polarizer and a polarization-maintaining circulator (PM-CIR), respectively. Both linearly-polarized pump and probe waves were launched into the near end of the PMF through two orthogonal ports of PBS/C1, so that pump and probe waves propagated along the PMF with orthogonal polarization states. At the far end of the PMF, two ports of PBS/C2 were spliced together with a PM-ISO. The optical output from the PM-CIR was attenuated by a variable optical attenuator (VOA) and detected by a photo-detector (PD). The electrical signal was demodulated by a lock-in amplifier (LIA) at the chopping frequency of 123 kHz. The demodulated signal was sampled by a data acqusition card (DAQ) as a function of the microwave frequency (ν) to collect the Brillouin gain spectrum (BGS) at the position corresponding to the correlation peak. By adjusting the modulation frequency $f_{\rm m}$, the position of the correlation peak was shifted along the PMF to get the distribution of BGS.

B. cm-Order Spatial Resolution

We set the modulation frequency $f_{\rm m}$ to 470. 134–528.968 kHz, which corresponds to a nominal measurement range $d_{\rm m} =\sim 200$ m and a nominal spatial resolution $\Delta z = 16$ cm according to (1) and (2), respectively. As schematically shown in Fig. 3(a), a 200-m-length PMF sample was constructed, which comprises four portions (A, B, D, and E) heated by a hot plate and two portions (C and F) strained by two sets of x-stages, respectively. All heated or strained portions were about 16–20 cm in length.

Fig. 3(b) depicts the characterized BFS $(\nu_{\rm B})$ distribution along the PMF when the temperature of the heated portions was set to $T = 81°$C. According to the repeatability test at a single position, the accuracy of the BFS $(\nu_{\rm B})$ measurement was about ± 3 MHz. One example of the three-dimensional (3-D) plot of the distributed BGS around the input end of the PMF is shown in Fig. 3(c) where the increased BFS $\nu_{\rm B}$ in the heated D and E portions can be clearly seen. The magnified views of the BFS $(\nu_{\rm B})$ distribution around all the heated portions are depicted in the insets of Fig. 3(b). It is validated that the measurement range of our novel scheme is kept the same as the traditional BOCDA system. We repeated the BGS measurement along the PMF when the temperature of the heated portions was set to different value. The BFS $(\nu_{\rm B})$ distribution around the input end of the PMF is plotted in Fig. 4(a). The small fluctuation of the characterized BFS $(\nu_{\rm B})$ around the heated portions seems to come from the bending stress when placed on the hot plate. It is noted that the BFS $(\nu_{\rm B})$ distribution varies by about 20 MHz when the temperature (T) is higher than 81°C, which is possibly due to the irregular heating upon the fiber portions attached to the hot plate and the heating-induced bending stress. We extracted the BFS $(\nu_{\rm B})$ at the centers of the heated portions and summarized it as a function of temperature in Fig. 4(b). The temperature coefficient was characterized by linear fitting

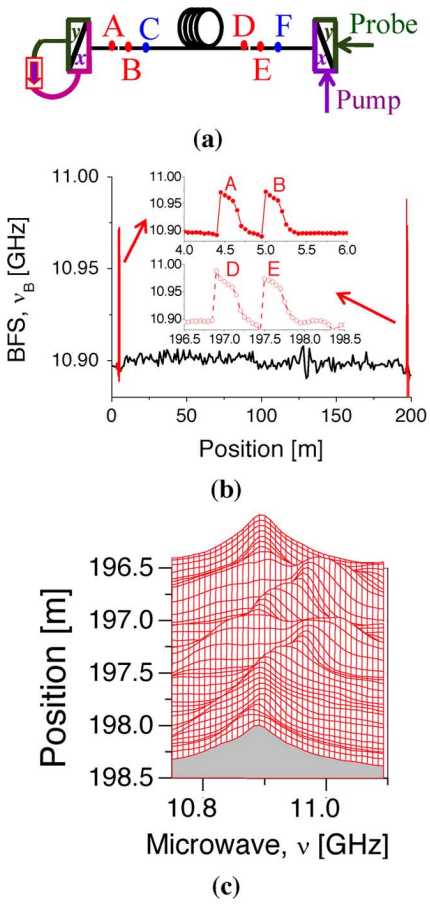

Fig. 3. (a) Prepared 200-m PMF sample with four heated portions (A, B, D, and E) and two strained portions (C and F). (b) Measured BFS (ν_B) distribution when the temperature of the heated portions is $T = 81°C$. The insets show the results around the heated portions. The accuracy of BFS (ν_B) measurement at a single position was about ± 3 MHz. (c) 3-D plot of the distributed BGS around the near end of the PMF.

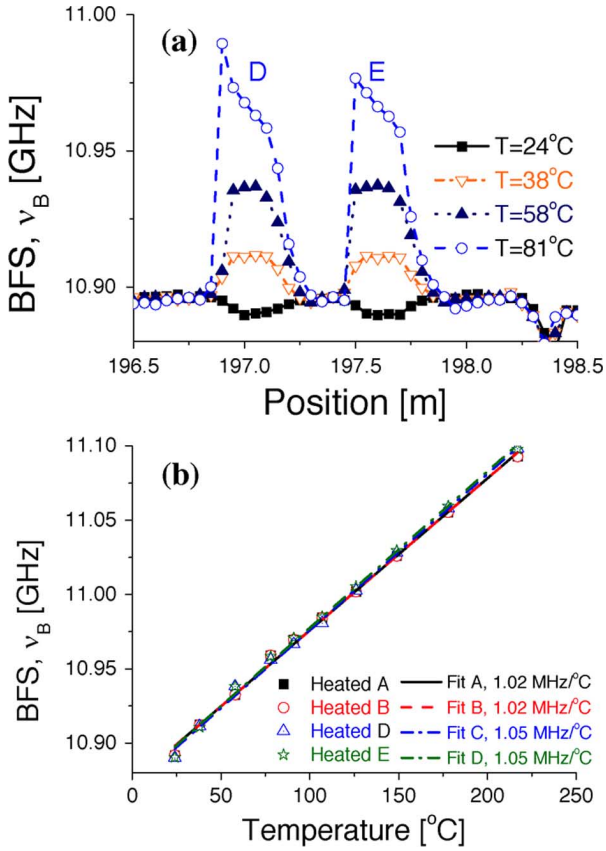

Fig. 4. (a) Measured BFS (ν_B) distribution around the near end of the PMF when the temperature of the heated portions is set to different value. (b) Characterized BFS (ν_B) dependence on temperature at each heated portion.

to the experimental data. The average temperature coefficient over all the heated portions is ~ 1.03 MHz/°C, which is in excellent agreement with the result over an entire 32-m PMF [12]. Considering the accuracy of the BFS (ν_B) measurement, the temperature accuracy was estimated to be about $\pm 3°C$.

When ~ 0.3-% strain was applied to the C and F portions, we measured the BGS and BFS (ν_B) distributions again. The BFS distribution is depicted in Fig. 5(a) and the 3-D plot of the distributed BGS around the near end of the PMF is shown in Fig. 5(b). As shown in Fig. 5(b) or the inset of Fig. 5(a), the strain-increased BFS ν_B is clearly recognized. The non-uniform distribution of the characterized BFS seems to come from the mitigation effect by the bonding epoxy and the fiber jacket. After applying different strain on the C and F portions, we characterized the BFS at the center of the strained portions as a function of strain. The experimental result at each strained portion is summarized in Fig. 5(c). The average strain coefficient (~ 0.045 MHz/$\mu\varepsilon$) matches also well with the result over an entire 32-m PMF [12]. The strain accuracy was estimated to be about ± 66 $\mu\varepsilon$.

It is noted that the interrogated BFS (ν_B) becomes incorrect when the applied strain is beyond ~ 6000 $\mu\varepsilon$. The inset of Fig. 5(c) depicts an example of the measured BGS when the applied strain is ~ 6625 $\mu\varepsilon$. The local BGS at the sensing (correlation peak) position [see the right-hand part of the inset of Fig. 5(c)] has a Lorentzian-shaped profile; the BGS accumulated along the uncorrelated positions [see the left-hand part of the inset of Fig. 5(c)] has two spread-out peaks due to the nature of sinusoidal frequency modulation of the laser source (see the optical spectrum depicted in the inset of Fig. 2). The local BGS at the sensing position locates far away from the accumulated BGS along the other positions due to the heavily-applied strain so that the Lorentzian-shaped profile is buried by the two spread-out peaks. Consequently, the BFS (i.e., the applied strain) would be falsely interrogated as one of two peaks of the accumulated BGS, as shown in the Fig. 5(c). However, when the strain is below ~ 6000 $\mu\varepsilon$, the local BGS at the sensing strain locates close to the accumulated BGS, which keeps the measured BGS the sharp Lorentizan-shaped profile, which can be clearly seen from Fig. 3(c) or 5(b). The above features limit the maximum measurable strain (~ 6000 $\mu\varepsilon$) although it can be improved to some extent by modifying the optical spectrum of the laser source [19].

Additionally, we demonstrated 5-cm spatial resolution by setting the modulation frequency f_m to 1813.61–1856.98 kHz. The nominal d_m and Δz were estimated to be 56 m and 5 cm according to (1) and (2), respectively. In experiment, we succeeded in measuring the strain- and temperature-induced BFS (ν_B) changes in ~ 5-cm portions. The accuracy of the BFS (ν_B)

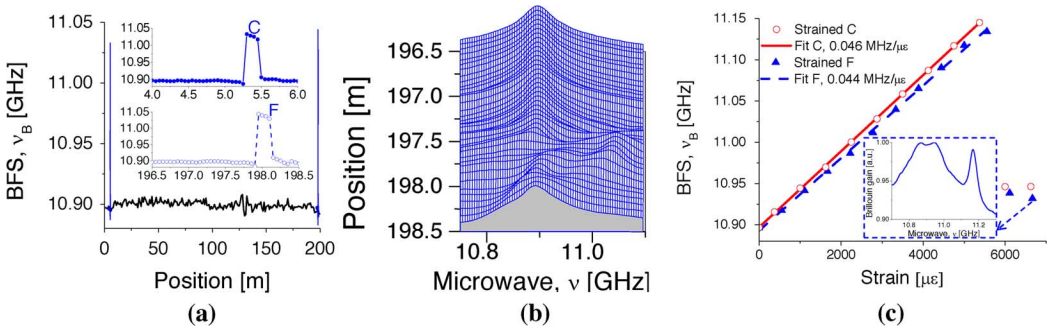

Fig. 5. (a) Measured BFS (ν_{B}) distribution when $\sim$0.3-% strain is applied to both C and F portions. The insets show the results around the strained portions. The accuracy of BFS (ν_{B}) measurement at a single position was about ± 3 MHz. (b) 3-D plot of the distributed BGS around the input end of the PMF. (c) Characterized BFS (ν_{B}) dependence on strain at each strained portion. The inset shows the local BGS at the strained F portion when the strain is $\sim 6625\ \mu\varepsilon$.

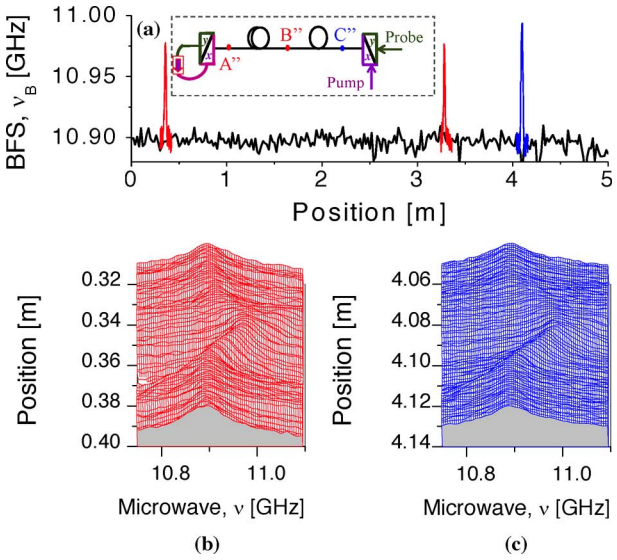

Fig. 6. (a) Measured BFS (ν_{B}) distribution along the 5-m PMF sample. The inset shows the PMF sample with two heated portions (A$''$ and B$''$) and one strained portion (C$''$). The accuracy of BFS (ν_{B}) measurement at a single position was about ± 5 MHz. 3-D plot of the distributed BGS around the heated A$''$ portion (b) and the strained C$''$ portion (c).

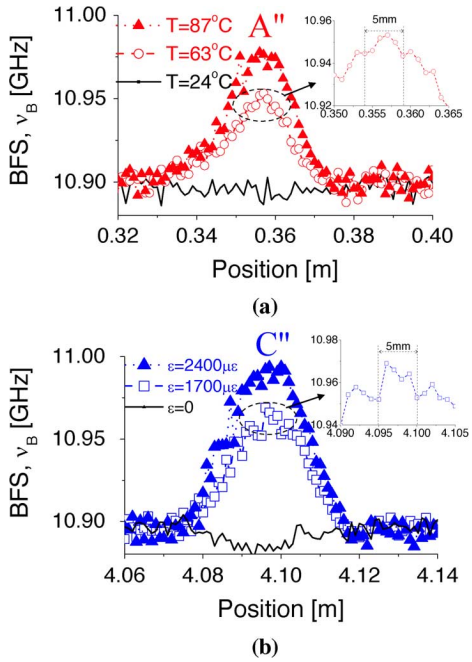

Fig. 7. Measured BFS (ν_{B}) distribution around the heated A$''$ portion (a) and the strained C$''$ portion (b). The accuracy of BFS (ν_{B}) measurement at a single position was about ± 5 MHz. The insets show the magnified views around the centers of heated and strained portions.

measurement at a single position was about ± 3 MHz, corresponding to the strain accuracy of $\pm 66\ \mu\varepsilon$ and the temperature accuracy of about ± 3°C, respectively.

C. Sub-cm Spatial Resolution

Finally, we demonstrate distributed sensing of temperature or strain with a spatial resolution of 5 mm, which is the highest value reported to date in all single-end-access Brillouin-based distributed sensors. The largest $\Delta f =\sim 12$ GHz of the DFB-LD was applied; the modulation frequency f_{m} was set to 18.468–18.525 MHz near the Brillouin linewidth $\Delta\nu_{\mathrm{B}}$. According to Eqs (1) and (2), the nominal d_{m} and Δz were calculated to be 5.6 m and 5 mm, respectively.

As schematically illustrated in the inset of Fig. 6(a), the prepared 5-m PMF sample comprises two 5-mm portions (A" and B") and one 5-mm strained portion (C$''$). The heated portions were bended and attached on the hot plate; the strained portion was fixed on a set of x-stages by 2-cm bonding epoxy at each side. The measured BFS (ν_{B}) distribution along the 5-m PMF sample when $T = 87$°C and $\Delta\varepsilon = 0.24\%$ is plotted in Fig. 6(a). The BFS (ν_{B}) increments induced by the temperature increment and the applied strain are obviously visible. The BGS distributions around the two ends of the PMF are depicted in Figs. 6(b) and (c), respectively.

When different ΔT or $\Delta\varepsilon$ was applied, we repeated the distributed measurements. The experimental results of the BFS (ν_{B}) distributions around the A" and C" portions are summarized in Fig. 7(a) and (b), respectively. The accuracy of the BFS measurement at a single position was about ± 5 MHz, corresponding to the strain accuracy of $\pm 110\ \mu\varepsilon$ and the temperature accuracy of about ± 5°C. It is shown that different BFS change induced by different ΔT or $\Delta\varepsilon$ can be clearly derived.

It is observed that a triangle-shaped distribution of the BFS is slightly asymmetric in each measurement [see Fig. 7(a)], which possibly originates from the asymmetric bending effect around the heated portions. A triangle-shaped distribution of the BFS is also observed in Fig. 7(b). This is because the applied strain

on the 5-mm fiber portion is gradually released along both sides of the bonding epoxy. The BFS at the nominal 0 $\mu\varepsilon$ is below the baseline level around the strained portion, which is possibly attributed to the compressed stress by two bonding epoxy when x-stages are set at the nominal 0 $\mu\varepsilon$. The insets are the magnified views around the centers of the heated and strained portions. Gradual but distinctive variations of the BFS can be seen near the heated portion (illustrated by dashed lines), which substantially shows the spatial resolution of about 5 mm.

IV. Conclusion

We have demonstrated a novel single-end-access SBS-based distributed sensor. By combining a PMF with two PBS/C's and one PM-ISO as a sensing unit, both pump and probe waves are input into the same end of the PMF to obtain the distributed temperature or strain information. Superior to the previously-proposed method based on a reflector [9], the measurement range of the new scheme is kept the same as the traditional BOCDA system; neither an optical filter nor a beat-lock-in detection is necessary for demodulation of the amplified probe signal; the frequency modulation depth can be larger than a half of the BFS ν_{B} ensuring higher spatial resolution. By setting different modulation frequency (f_{m}) to the laser source, we have experimentally demonstrated distributed sensing with three different alternatives of the measurement range to the spatial resolution $(d_{\mathrm{m}}/\Delta z)$ of 200 m/16 cm, 56 m/5 cm, and 5.6 m/5 mm, respectively. Further combination with our recent proposed complete discrimination of strain and temperature based on a PMF [12] will provide a technique of single-end-access distributed discriminative sensing of strain and temperature, which is now in the plan.

The utilization of a PMF as the sensing fiber offers ideal SBS interaction between Brillouin pump and probe waves with the same polarization states (x-oriented in this study) while the system based on a PMF needs a higher cost than that based on a SMF. The current demonstration is limited to a measurement range of 200 m at 16-cm spatial resolution although the ratio of $d_{\mathrm{m}}/\Delta z$ is expectable to be further improved by employing a laser diode with a broader modulation depth [5] or by using a temporal-gating technique [20]. However, considering the increased crosstalk of the PMF, the measurement range is hardly achievable to be more than 1 km.

References

[1] X. Bao, D. J. Webb, and D. A. Jackson, "32-km distributed temperature sensor using Brillouin loss in optical fiber," *Opt. Lett.*, vol. 18, no. 18, pp. 1561–1563, Sep. 1993.

[2] M. Nikles, L. Thevenaz, and P. Robert, "Simple distributed sensor based on Brillouin gain spectrum analysis," *Opt. Lett.*, vol. 21, no. 10, pp. 758–760, May 1996.

[3] M. N. Alahbabi, Y. T. Cho, and T. P. Newson, "150-km-range distributed temperature sensor based on coherent detection of spontaneous Brillouin backscatter and in-line Raman amplification," *J. Opt. Soc. Amer. B*, vol. 22, no. 6, pp. 1321–1324, Jun. 2005.

[4] K. Hotate and T. Hasegawa, "Measurement of Brillouin gain spectrum distribution along an optical fiber using a correlation-based technique—Proposal, experiment and simulation," *IEICE Trans. Electron.*, vol. E83-C, no. 3, pp. 405–412, Mar. 2000.

[5] K. Y. Song, Z. He, and K. Hotate, "Distributed strain measurement with millimeter-order spatial resolution based on Brillouin optical correlation domain analysis," *Opt. Lett.*, vol. 31, no. 17, pp. 2526–2528, Sep. 2006.

[6] Y. Mizuno, W. Zou, Z. He, and K. Hotate, "Proposal of Brillouin optical correlation-domain reflectometry (BOCDR)," *Opt. Exp.*, vol. 16, no. 16, pp. 12148–12153, Aug. 2008.

[7] T. Horiguchi, T. Kurashima, and M. Tateda, "Tensile strain dependence of Brillouin frequency shift in silica optical fibers," *IEEE Photon. Technol. Lett.*, vol. 1, no. 5, pp. 107–108, May 1989.

[8] W. Zou, Z. He, and K. Hotate, "Investigation of strain- and temperature-dependences of Brillouin frequency shifts in GeO_2-doped optical fibers," *J. Lightw. Technol.*, vol. 26, no. 13, pp. 1854–1861, Jul. 2008.

[9] K. Y. Song and K. Hotate, "Brillouin optical correlation domain analysis in linear configuration," *IEEE Photon. Technol. Lett.*, vol. 20, no. 24, pp. 2150–2152, Dec. 2008.

[10] K. Y. Song, W. Zou, Z. He, and K. Hotate, "All-optical dynamic grating generation based on Brillouin scattering in polarization-maintaining fiber," *Opt. Lett.*, vol. 33, no. 9, pp. 926–938, May 2008.

[11] W. Zou, Z. He, and K. Hotate, "Two-dimensional finite element modal analysis of Brillouin gain spectra in optical fibers," *IEEE Photon. Technol. Lett.*, vol. 18, no. 23, pp. 2487–2489, Dec. 2006.

[12] W. Zou, Z. He, and K. Hotate, "Complete discrimination of strain and temperature using Brillouin frequency shift and birefringence in a polarization-maintaining fiber," *Opt. Exp.*, vol. 17, no. 3, pp. 1248–1255, Feb. 2009.

[13] W. Zou, Z. He, K. Y. Song, and K. Hotate, "Correlation-based distributed measurement of dynamic grating spectrum generated in stimulated Brillouin scattering in a polarization-maintaining optical fiber," *Opt. Lett.*, vol. 34, no. 7, pp. 1126–1128, Apr. 2009.

[14] W. Zou, Z. He, and K. Hotate, "Demonstration of Brillouin distributed discrimination of strain and temperature using a polarization-maintaining optical fiber," *IEEE Photon. Technol. Lett.*, vol. 22, no. 8, pp. 526–528, Apr. 2010.

[15] K. Y. Song, W. Zou, Z. He, and K. Hotate, "Optical time-domain measurement of Brillouin dynamic grating spectrum in a polarization-maintaining fiber," *Opt. Lett.*, vol. 34, no. 9, pp. 1381–1383, May 2009.

[16] K. Y. Song and H. J. Yoon, "High-resolution Brillouin optical time domain analysis based on Brillouin dynamic grating," *Opt. Lett.*, vol. 35, no. 1, pp. 52–54, Jan. 2010.

[17] K. Y. Song, S. Chin, N. Primerov, and L. Thevenaz, "Time-domain distributed sensor with 1 cm spatial resolution based on Brillouin dynamic gratings," in *Proc. 20th Int. Conf. Optical Fibre Sensors*, Edinburgh, U.K., Oct. 2009, vol. 5703, Paper PDP-01.

[18] G. P. Agrawal, *Nonlinear Fiber Optics*, 3rd ed. New York: Academic, 2001.

[19] K. Y. Song, Z. He, and K. Hotate, "Optimization of Brillouin optical correlation domain analysis system based on intensity modulation scheme," *Opt. Exp.*, vol. 14, no. 10, pp. 4256–4263, May 2006.

[20] M. Kannou, S. Adachi, and K. Hotate, "Temporal gating scheme for enlargement of measurement range of Brillouin optical correlation domain analysis for optical fiber distributed strain measurement," in *Proc. 16th Int. Conf. Optical Fiber Sensors*, 2003, pp. 454–457.

Weiwen Zou (S'05–M'08) was born in Jiangxi, China, on January 3, 1981. He received the B.S. degree in physics and M.S. degree in optics from Shanghai Jiao Tong University, China, in 2002 and 2005, respectively, and the Ph.D. degree in optoelectronics from the University of Tokyo, Tokyo, Japan, in 2008.

In 2003, he was engaged in research of non-volatile photorefractive-based holography with the University of Electro-Communications, Japan, as an exchange student. Since 2005, he has been working on Brillouin-scattering-based discriminative sensing of strain and temperature for his doctoral research in electronic engineering, the University of Tokyo. From 2008 to 2009, he was a Postdoctoral Research Fellow with the University of Tokyo. In 2009, he became a Project Assistant Professor with the University of Tokyo. In 2010, he joined Shanghai Jiao Tong University, Shanghai, China, as an Associate Professor. His current research interests include fiber-optic distributed sensors, fiber-optic measurement, and optical information processing.

Dr. Zou is a member of the Optical Society of America.

Zuyuan He (M'00) received the B.S. and M.S. degrees in electronic engineering from Shanghai Jiao Tong University, Shanghai, China, in 1984 and 1987, respectively, and the Ph.D. degree in optoelectronics from the University of Tokyo, Tokyo, Japan, in 1999.

He joined Nanjing University of Science and Technology, Nanjing, China, as a Research Associate in 1987, and became a Lecturer in 1990, where he was engaged in the research of fiber optic sensors, evaluation and measurement of optical devices, and optical instrumentation. From 1995 to 1996, he was a Research Fellow studying on optical information processing in the Research Center for Advanced Science and Technology (RCAST), University of Tokyo. In 1999, he became a Research Associate of the University of Tokyo, where he worked on measurement and characterization of fiber optic components and systems, fiber optic reflectometry, fiber optic sensors, and multi-dimensional optical information processing. In 2001, he joined CIENA Corporation, Linthicum, MD, as a Lead Engineer responsible for optical testing and optical process development. He returned to the University of Tokyo as a Lecturer in 2003, and became an Associate Professor in 2005. He is now a Professor with the Center of Excellence in Electrical and Electronic Engineering, University of Tokyo. His current research interests include optical fiber sensors, optical fiber measurement, and optical information processing.

Dr. He is a member of the Optical Society of America and the Institute of Electronics, Information, and Communication Engineers (IEICE) of Japan.

Kazuo Hotate (M'91–SM'98–F'03) was born in Tokyo, Japan, on June 20, 1951. He received the B.E., M.E., and Dr. Eng. degrees in electronic engineering from the University of Tokyo, Tokyo, Japan, in 1974, 1976, and 1979, respectively.

In 1979, he joined the University of Tokyo as a Lecturer. He became a Professor in 1993 at the Research Center for Advanced Science and Technology (RCAST), University of Tokyo. Currently, he is a Professor with the Department of Electrical Engineering and Information Systems, School of Engineering, University of Tokyo. He served as the Dean of Faculty and Graduate School of Engineering, University of Tokyo, in 2008 and 2009. He was engaged in projection-type holography, measurement and analysis of optical fiber characteristics. He served as the co-chairs for SPIE Fiber Optic Gyros: Twentieth Anniversary Conference (1996), the Technical Program Committee Chair for 13th International Conference on Optical Fiber Sensors (OFS-13) (1999), and the General Chair for OFS-16 (2003). At present, he is working on photonic sensing. He has authored and coauthored several books on optical fibers and optical fiber sensors and more than 370 journal papers and international conference presentations.

Prof. Hotate is a Fellow of Institute of Electronics, Information, and Communication Engineers (IEICE), the Society of Instrumentation and Control Engineers (SICE), and the Japan Society of Applied Physics (JSAP). He was a BoG member of the IEEE Photonic Society. He was the recipient of several academic awards, such as SPIE DSS Life-time Achievement Award, the Ichimura Prize, and the Hasunuma Prize (SICE).

202.120.19.89 [年 2018-03-05 00:07:48]